







RESEARCH ARTICLE

Robotic mapping of motor cortex in children with perinatal stroke and hemiparesis

Hsing-Ching Kuo^{1,2,3,4,5}  | Ephrem Zewdie^{1,2,3,4}  | Adrianna Giuffre^{1,2,3,4}  |
Liu Shi Gan³ | Helen L. Carlson^{1,2,3,4}  | James Wrightson^{1,2,3,4}  |
Adam Kirton^{1,2,3,4} 

¹Calgary Pediatric Stroke Program, University of Calgary, Calgary, Alberta, Canada

²Alberta Children's Hospital Research Institute (ACHRI), Calgary, Alberta, Canada

³Hotchkiss Brain Institute (HBI), Calgary, Alberta, Canada

⁴Department of Pediatrics and Clinical Neurosciences, Cumming School of Medicine, University of Calgary, Calgary, Alberta, Canada

⁵Department of Physical Medicine & Rehabilitation, University of California Davis, Sacramento, California, USA

Correspondence

Adam Kirton, Calgary Pediatric Stroke Program, University of Calgary, 28 Oki Drive NW, Calgary AB T3B6A8, Canada.
Email: adam.kirton@ahs.ca

Funding information

Alberta Children's Hospital Research Institute; Canadian Institutes of Health Research; Canadian Partnership for Stroke Recovery, Grant/Award Number: Postdoctoral Award

Abstract

Brain stimulation combined with intensive therapy may improve hand function in children with perinatal stroke-induced unilateral cerebral palsy (UCP). However, response to therapy varies and underlying neuroplasticity mechanisms remain unclear. Here, we aimed to characterize robotic motor mapping outcomes in children with UCP. Twenty-nine children with perinatal stroke and UCP (median age 11 ± 2 years) were compared to 24 typically developing controls (TDC). Robotic, neuronavigated transcranial magnetic stimulation was employed to define bilateral motor maps including area, volume, and peak motor evoked potential (MEP). Map outcomes were compared to the primary clinical outcome of the Jebsen–Taylor Test of Hand Function (JTT). Maps were reliably obtained in the contralesional motor cortex (24/29) but challenging in the lesioned hemisphere (5/29). Within the contralesional M1 of participants with UCP, area and peak MEP amplitude of the unaffected map were larger than the affected map. When comparing bilateral maps within the contralesional M1 in children with UCP to that of TDC, only peak MEP amplitudes were different, being smaller for the affected hand as compared to TDC. We observed correlations between the unaffected map when stimulating the contralesional M1 and function of the unaffected hand. Robotic motor mapping can characterize motor cortex neurophysiology in children with perinatal stroke. Map area and peak MEP amplitude may represent discrete biomarkers of developmental plasticity in the contralesional M1. Correlations between map metrics and hand function suggest clinical relevance and utility in studies of interventional plasticity.

KEYWORDS

cerebral palsy, motor mapping, perinatal stroke, plasticity, robotic TMS, transcranial magnetic stimulation

This is an open access article under the terms of the [Creative Commons Attribution-NonCommercial-NoDerivs](https://creativecommons.org/licenses/by-nc-nd/4.0/) License, which permits use and distribution in any medium, provided the original work is properly cited, the use is non-commercial and no modifications or adaptations are made.

© 2022 The Authors. *Human Brain Mapping* published by Wiley Periodicals LLC.

1 | INTRODUCTION

Perinatal stroke is a focal vascular brain injury near the beginning of life (Dunbar & Kirton, 2019; Raju et al., 2007). It is the most common etiology of unilateral cerebral palsy (UCP) (Wu et al., 2006), affecting approximately 1:1000 live births (Dunbar et al., 2020; Raju et al., 2007) and millions of people globally (Oskoui et al., 2013). Such early brain injury interrupts typical development. Depending on lesion type, size, location, and many other factors, functional limitations after perinatal stroke may include motor deficits, sensory dysfunction, cognitive delay, language and speech impairment, and epilepsy (Kirton & Deveber, 2013). Such limitations result in life-long morbidity and decrease the quality of life of children and families.

UCP is the most common form of cerebral palsy (CP), with motor and sensory impairment lateralized to half of the body. The focal, unilateral lesions of perinatal stroke offer an ideal model for studying developmental neuroplasticity of the human motor system, with strong evidence from both animal and human mapping literature (Kirton et al., 2021; Martin et al., 2007, 2011; Staudt, 2007). In typical prenatal development, corticospinal projections from diffuse cortical areas connect to diffuse areas of spinal cord grey matter with approximately equal contralateral and ipsilateral connections. During early postnatal development, these connections are refined with most projecting from the primary motor cortex (M1) to the anterior horn of the contralateral spinal cord while ipsilateral projections are pruned. Perinatal stroke may alter this process, whereby corticospinal projections from the lesioned hemisphere lose their ability to compete for contralateral spinal synapses. This in turn may allow contralesional M1 projections to preserve their ipsilateral corticospinal projections to the affected hand (Kuo et al., 2017; Zewdie et al., 2017). The relative relationship between these contra- and ipsi-lateral corticospinal arrangements have been variably associated with hand function in children with UCP though the relationship is incompletely understood (Kuo et al., 2018; Riddell et al., 2019; Simon-Martinez et al., 2019; Smorenburg et al., 2017), suggesting additional developmental alterations in motor neurophysiology are occurring.

Categorical characterization of corticospinal organization as ipsilateral or contralateral is crude and unable to account for most of the variance in function in children with UCP (Friel et al., 2016; Marneweck et al., 2018). Motor maps are topographic representations that may reflect motor control of specific body parts (Penfield & Rasmussen, 1950). Motor map metrics such as area and volume may be useful biomarkers of functional impairment and recovery in animal studies (Milliken et al., 2013; Nudo & Milliken, 1996) and in adult stroke (Grefkes & Ward, 2014). Specifically, animal studies suggested that motor map territory can be a valuable neurophysiological measure for quantifying the neural substrate topography and plasticity associated with functional change due to brain injury or motor skill training (Nudo & Milliken, 1996; Nudo, Milliken, et al., 1996; Nudo, Wise, et al., 1996). Important findings pertinent to rehabilitation include observations that skill training-induced improvements in motor function can be accompanied by expansion of map area and normalization of corticospinal neuron distribution in the spinal cord (Friel et al., 2000, 2012; Kleim et al., 1998).

While map territories have been measured with intracortical electrophysiology in animals, noninvasive and painless transcranial magnetic stimulation (TMS) provides similar opportunity in humans and has been used extensively in adult stroke patients to better understand recovery, training effects, and function (Thickbroom et al., 2004; Yarossi et al., 2019). TMS experience in the developing brain appears to be safe and well tolerated (Zewdie et al., 2020) with valuable applications in CP populations. Kesar et al. (2012) showed that the geometric location of peak motor activations may be displaced, the degree of which is associated with function in children with nonspecific CP. In a more homogeneous group of children with UCP, Friel et al. (2016) showed structured intensive bimanual training could expand motor map area and increase MEP amplitudes of the more-affected hand. These promising studies were not able to study specific disease-states such as perinatal stroke and were vulnerable to the challenges of performing manual TMS motor mapping in children. Robotic TMS systems may mitigate such challenges, affording near real-time localization of coil placement, reducing human technical errors, and decreasing experiment time. We have demonstrated the reliability (Giuffre et al., 2020) and feasibility of robotic TMS to map M1 neurophysiology in typically developing children (TDC; Giuffre et al., 2019, 2021; Grab et al., 2018). Robotic TMS has not been applied to children with perinatal brain injuries and CP.

Understanding the mechanisms of developmental plasticity that occur after perinatal stroke is germane to the development of novel therapies (Kirton et al., 2021). Early, randomized, controlled clinical trials of noninvasive brain stimulation suggest possible efficacy (Gillick et al., 2018; Kirton et al., 2017). Most trials have targeted the contralesional hemisphere, but precise targets and mechanisms of interventional plasticity remain poorly defined. The importance of the entire contralesional hemisphere in determining clinical function in children with perinatal stroke is increasingly understood (Craig et al., 2020) but more refined models of the role of the primary motor cortex are required. Personalized maps of motor neurophysiology may also help identify optimal candidates for, and the interventional plasticity effects of, both traditional (e.g., constraint-induced) and neuromodulatory therapies. However, evidence to date suggests simple corticospinal tract organization (Friel et al., 2021) or more advanced imaging methods (Juenger et al., 2013) have a limited ability to do so, suggesting further possible utility of detailed, individualized motor maps.

Here, we aimed to employ robotic TMS motor mapping to define bilateral map characteristics and their association with clinical function in children with perinatal stroke-induced UCP. We hypothesized that motor map area of children with UCP would be smaller than that of TDC and that the motor map area would be positively correlated with hand function in children with UCP.

2 | METHODS

2.1 | Participants

Participants with perinatal stroke were recruited from the Alberta Perinatal Stroke Project, a population-based research cohort (Cole

et al., 2017) to participate in a rehabilitation clinical trial called SPORT (Stimulation for Perinatal Stroke Optimizing Recovery Trajectories, clinicaltrials.gov/NCT03216837). SPORT is an on-going, randomized, sham-controlled, double-blinded multicenter trial examining the efficacy of camp-based, child-centered intensive rehabilitation paired with tDCS. Baseline (preintervention) neurophysiology assessments included the motor mapping described here.

Inclusion criteria were: (1) age 6–18 years, (2) magnetic resonance imaging (MRI)-confirmed perinatal ischemic stroke (neonatal arterial ischemic stroke, NAIS; arterial presumed perinatal ischemic stroke, APPIS; or periventricular venous infarction, PVI; Dunbar & Kirton, 2018), (3) symptomatic hemiparetic CP, including parent/child perceived limitations in function with disability severity that allows lifting the affected arm above a table surface and some ability to grasp light objects, (4) term birth (>36 weeks), (5) written informed consent/assent. Exclusion criteria were: additional neurological abnormality not related to perinatal stroke, multifocal stroke, severe hemiparesis (MACS V), severe spasticity (Modified Ashworth Scale >3), severe developmental delay precluding compliance to experiment procedures, unstable epilepsy, any TMS or MRI contraindications, and orthopedic surgery, botulinum toxin, constraint, brain stimulation, or other modulatory therapy in past 6 months.

Typically developing controls (TDC) were recruited to participate in the AMPED (accelerated motor learning in PEDIiatrics) trial to examine the effects of high-definition and conventional tDCS on motor learning in children (Cole et al., 2018). AMPED was a randomized, double-blinded, sham-controlled clinical trial (clinicaltrials.gov/NCT03193580). Briefly, children who were between 12 and 18 years of age, right-handed, and of typical neurodevelopment without major medical conditions or TMS/MRI contraindications were recruited. The baseline (preintervention) mapping results are used as the comparison group for the current study. The methods used for MRI and TMS mapping were identical for both children with perinatal stroke and TDC.

2.2 | Magnetic resonance imaging

MRI was performed at Alberta Children's Hospital Diagnostic Imaging Suite using a 3T General Electric MR750w scanner (GE Healthcare, Chicago, IL). High resolution T1-weighted anatomical images were obtained using fast spoiled gradient echo sequence (FSPGR BRAVO, 226 contiguous axial slices, repetition time = 8.5 ms, echo time = 3.2 ms, voxels = 1 mm isotropic, duration ~5 min). Individual T1 structural images were utilized in the TMS neuronavigation software, described below.

2.3 | TMS motor mapping

TMS motor mapping was conducted at the Pediatric Non-invasive Neurostimulation Laboratory at the Alberta Children's Hospital in Calgary Canada. Robotic TMS (Axilum Robotics, France) was utilized to

perform all motor mapping procedures, the details of which are described elsewhere (Giuffre et al., 2019; Grab et al., 2018) and below. The Axilum TMS robot accommodates a 70-mm Air-Film coil (Magstim, UK), allows precise neuronavigation, near real-time motion correction, and compensates for human operation errors associated with manual mapping (Goetz et al., 2019).

Neuronavigation (Brainsight2, Rogue Research, Montréal) was used to reconstruct skin and curvilinear brain, to generate stimulation grids and targets (details below), and to record stimulation trials. The neuronavigation software enables maintenance of stimulation target alignment tangentially to the reconstructed scalp and stimulation trajectories projected perpendicular to the cortical target. Adjustments of individual trajectories were sometimes required, especially in participants with large brain lesions. Coil orientation was maintained by the robotic system at a 45° angle to the interhemispheric fissure to produce posterior–anterior current.

Following participant orientation, a pair of Ag-AgCl electrodes (Kendall, Chicopee, MA) were applied to record surface electromyogram (EMG) from the first dorsal interosseous (FDI) muscles bilaterally with a ground electrode on the wrist styloid process. EMG signals were amplified (gain = 1000, Bortec Biomedical, Calgary), band-pass filtered (20–2500 Hz) and then digitized at a rate of 5000 Hz using CED 1401 hardware and Signal 6.0 software (Cambridge Electronic Design Limited). Raw EMG data were displayed on a computer screen to allow online monitoring by investigators. Participants were seated comfortably in the robot chair with both arms resting on a cushioned support, watched a movie among a selection in our laboratory, and encouraged to take breaks when needed.

Experiments began by mapping the contralesional (intact) motor cortex of children with UCP and the right hemisphere in TDC. Stimulations were first delivered in proximity to the anatomical hand knob to identify the “hotspot” of the contralateral FDI; the location producing the largest and most consistent MEP. This location was subsequently marked using the neuronavigation software and used for determining the resting motor threshold (RMT). Details for determining RMT were described in details in Giuffre and colleagues (Giuffre et al., 2021). Briefly, RMT was estimated from a stimulus response curve (SRC) which was produced by delivering four stimuli at 100% maximum stimulator output (%MSO) and then decreasing in 5% increments until no MEPs >50 μ V were observed. For children with UCP whose input–output data did not fit a sigmoidal input–output curve, a conventional RMT thresholding method was performed. Intensity was adjusted with increments of 2%MSO based on the MEP responses to determine the minimal intensity inducing MEP >50 μ V in >5/10 trials. The same thresholding procedure was then performed for the ipsilateral, affected FDI within the contralesional hemisphere.

Modified procedures to localize the contralateral FDI hotspot were performed for the lesioned hemisphere in children with UCP. For participants with arterial stroke, the anatomical hand knob may have been absent or altered. In such cases, task-based functional MRI peak activation location (during performance of a squeeze ball task as described elsewhere (Baker et al., 2020) was marked and used as a reference in the neuronavigation software. The perilesional area was

probed for any location producing the largest and most consistent MEP.

A customized rectangular grid (13 × 13 grid-points, 0.7-cm spacing) was then created and centered at the hand knob area (or the task-based fMRI activation location if the anatomy was altered) of individual participant's MRI. Four single-pulses were delivered at 120% of the RMT at 1-s inter-stimulus intervals to each grid point that allows acceptance or rejection of individual MEPs using the robotic TMS system (contralesional M1, $n = 20$, lesioned M1, $n = 7$). For children who were not able to tolerate such frequency of pulses, the inter-stimulus interval was adjusted to 5–10 s. A serial progression across the grid was employed to define each map as described previously (Giuffre et al., 2019, 2021; Grab et al., 2018). Beginning with the hotspot location, the coil was then moved anteriorly or posteriorly until no MEP responses were observed. The same approach was then completed in the medial to lateral plane in the neighboring grid row and repeated until a border of nonresponsive sites (<2/4 stimulations producing a MEP >50 μV) was established. If the RMT of the affected FDI differed from the unaffected FDI by >5%MSO, the contralesional M1 was mapped at two stimulator intensities, with each intensity corresponding to 120% of RMT of the affected or unaffected FDI.

Similar procedures were utilized for mapping in TDC, except for that the robotic TMS system always delivered four pulses at 120% RMT at 1 Hz to each grid point.

2.4 | TMS data analysis and motor maps

EMG sweeps were inspected visually during online data acquisition; trials were excluded when background signals were above 50 μV or when children were moving and repeated until a clean recording was obtained. EMG data were exported offline and subsequently analyzed using in-house scripts (MATLAB R2016b, The MathWorks, Inc., Natick, MA). Recordings with background EMG signal (10–30 ms prior to the TMS pulse) >50 μV were considered as facilitated and were discarded. MEPs >50 μV occurring 20–80 ms after the TMS pulse were

included. Peak-to-peak MEP amplitude was averaged across valid trials at each responsive site.

Individualized two-dimensional (2D) heatmaps and three-dimensional (3D, x-y-MEP; where x-axis is parallel to the central sulcus and y-axis is parallel to the interhemispheric fissure) motor maps were generated and overlaid on individual MRIs (Figures 1 and 2). Based on previous experience (Grab et al., 2018), a minimally acceptable number of responsive sites was determined to be ≥ 9 .

The primary motor mapping outcome was motor map area, calculated as the number of responsive sites (grids) multiplied by one grid area (0.7-cm × 0.7-cm = 0.49 cm²). Secondary mapping outcomes included the following:

1. Peak MEP amplitude of the 3D map, defined as the maximum averaged peak-to-peak MEP of the entire map.
2. Map volume, calculated as the cumulative sum of the peak-to-peak MEP amplitude at each grid-location multiplied by map area (0.49 cm²).

2.5 | Clinical assessments

For children with perinatal stroke, three standardized, validated upper extremity functional assessments were administered and scored by qualified pediatric occupational therapists. The Jebsen–Taylor Test of Hand Function (JTT) evaluated the speed of unimanual hand function by recording the duration (in seconds) of completing simple tasks. The child-friendly version included six components of daily activities, including card flipping, picking up and dropping of small objects, checker stacking, grasping and releasing light and heavy cans, and simulated eating (Beagley et al., 2016; Jebsen et al., 1969). To avoid frustration, when participants had difficulty completing the task within a given 2-min duration, the duration for that task was marked as 120 s (Duncan et al., 1998). Higher scores on the JTT reflect poorer performance. The Box and Blocks Test (BBT) evaluated unimanual dexterity by measuring how many blocks a participant can pick up, move over a

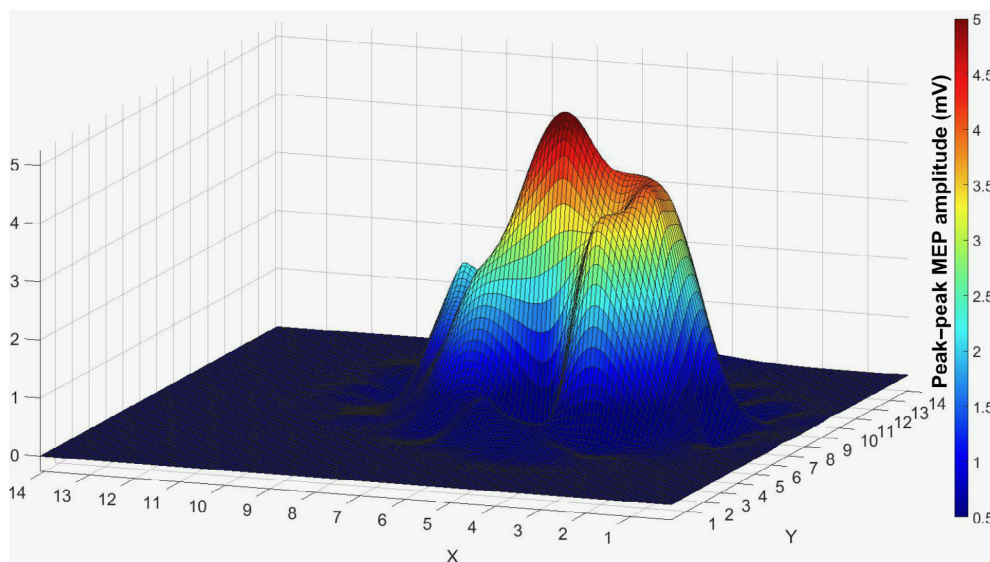


FIGURE 1 A typical example of a three-dimensional (3D) motor map. X and y axes are the coordinates from the mapping grid and the z axis represents the peak-to-peak averaged motor evoked potential (MEP) amplitude at the corresponding grid location. Color bar on the right represents the size of the MEP amplitude

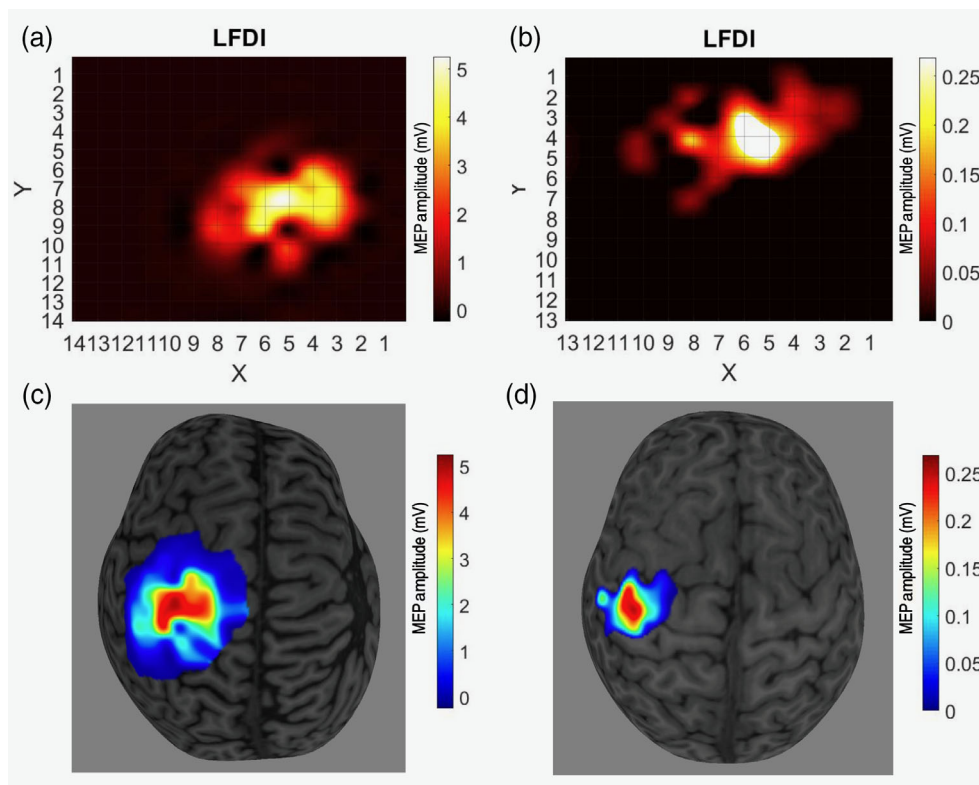


FIGURE 2 Representative motor maps in the contralesional motor cortex in children with perinatal stroke-induced unilateral cerebral palsy (UCP). (a) two-dimensional (2D) heat map of the affected (ipsilateral) first dorsal interosseus (FDI) from stimulating contralesional motor cortex. (c) This map is overlaid on the participant's magnetic resonance imaging (MRI). Both sub-figures (a,c) represent the same child who has AIS. (b) Another 2D heat map of the affected FDI from stimulation of the contralesional motor cortex. (d) This map is overlaid on another participant's MRI. Both sub-figures (b,d) represent the same child who has periventricular venous infarction (PVI). (d). Color bar represents the size of the MEP amplitude. Note that given the peak MEP amplitudes were very different between the two individuals (4.62 vs. 0.25 mV), we presented different scales for these two children to show detailed map topography

barrier, and drop off with each hand within 1 min (Mathiowetz et al., 1985). Both JTT and BBT assessments are standardized and reliable assessment protocols in TDC and children with UCP (Araneda et al., 2019; Jongbloed-Pereboom et al., 2013; Reedman et al., 2016; Taylor et al., 1973). The Assisting Hand Assessment (AHA) evaluated upper extremity hand function in various bimanual play activities in children with hemiparesis (Krumlind-Sundholm et al., 2007). Scores are reported in AHA logit units (0–100). Higher scores on both BBT and AHA reflect better performance. The JTT was also administered to TDC (Cole et al., 2018; Giuffre et al., 2021). Note that we acknowledge the unaffected upper extremity should ideally be termed “less-affected” and the affected side “more-affected.” We use the terms “unaffected” and “affected” to keep the terms consistent in the manuscript.

2.6 | Safety and tolerability

We used a modified pediatric noninvasive stimulation safety and tolerability questionnaire to evaluate children's experiences of the robotic TMS session (Garvey et al., 2001; Zewdie et al., 2020). Children were asked to rank the experience of their TMS session against

other common childhood experiences (e.g., play a video game). Additionally, possible side effects associated with TMS (e.g., headache, neck pain) were also screened for the duration and intensity (mild, moderate, or severe) immediately following the session.

2.7 | Statistical analysis

Shapiro–Wilk test was used to test data normality. First, motor map variables were compared between bilateral FDI of the contralesional hemisphere in children with UCP using paired or independent *t*-tests and Wilcoxon signed-rank or Mann–Whitney *U* tests, where appropriate. Next, motor map variables were compared between groups using Kruskal–Wallis test with post hoc comparisons (Dunn's test). Pearson correlation coefficient and Spearman's rho were used to examine potential associations between motor map and clinical outcomes, where appropriate. As there were only five maps successfully obtained and created in the lesioned hemisphere in UCP, we reported only descriptive statistics and plotted individual map topography for this hemisphere. Prism 8.4.3 (GraphPad Software, La Jolla, CA) and R Studio were used to perform statistical analyses and create figures. Matlab was used to generate 2D and 3D motor maps. Brainsight2

was used to overlay motor maps on individual MRIs. Alpha level was set at .05. *p*-values from statistical tests were adjusted using Bonferroni correction for multiple tests, where appropriate.

3 | RESULTS

3.1 | Population

Twenty-nine participants with perinatal stroke were studied (age range: 7 years 7 months to 19 years; mean age (SD): 11 years 5 months (2 years 4 months); 13 females, 16 males; left hemisphere

stroke, *n* = 19, 66%). Twenty-four TDC (age range 12 years 4 months to 17 years 6 months; mean age (SD): 15 years 6 months (1 year 8 months); 13 females, 11 males) participated. Demographics for both groups are reported in Table 1.

3.2 | Motor map characteristics

Detailed motor mapping results of TDC were reported in Giuffre et al. (2021). Consistent MEP responses were evoked in the contralateral right FDI (RFDI) when stimulating the left hemisphere in all TDC. Three participants were not fully evaluated: two received only

TABLE 1 Demographic characteristics and clinical outcomes

	Children with perinatal stroke				Typically developing children		
	All participants (<i>n</i> = 29)	Children with a contralesional M1 motor map with MEP recorded in the unaffected FDI (<i>n</i> = 24)	Children with a contralesional M1 motor map with MEP recorded in the affected FDI (<i>n</i> = 15)	Children with a lesioned M1 motor map (<i>n</i> = 5)	All participants (<i>n</i> = 24)	Children with a left hemisphere motor map (<i>n</i> = 21) ^a	Children with a right hemisphere motor map (<i>n</i> = 21) ^b
<i>Demographics</i>							
Gender (female: male)	13:16	11:13	7:8	3:2	13:11	12:9	11:10
Age, y (mean ± SD)	11 ± 2	12 ± 2	12 ± 3	11 ± 1	16 ± 2	16 ± 2	16 ± 2
Stroke side (left brain:right brain)	19:10	15:9	9:6	3:2	—	—	—
Stroke type (arterial: periventricular infarction)	16:13	12:12	8:7	0:5	—	—	—
<i>Clinical outcome</i>							
Baseline AHA, AHA logit units (mean ± SD)	54 ± 16	55 ± 16	51 ± 14	56 ± 10	—	—	—
Baseline JTTHF, nondominant hand, s (mean ± SD)	242 ± 213 ^c	225 ± 206 ^c	246 ± 217 ^c	113 ± 74	31.1 ± 4.9	31.2 ± 4.8	31.2 ± 5.3
Baseline BBT, more-affected hand, blocks/min (mean ± SD)	24 ± 13 ^c	25 ± 13 ^c	23 ± 13 ^c	31 ± 10	—	—	—
Baseline BBT, less-affected hand, blocks/min (mean ± SD)	51 ± 10 ^c	53 ± 10 ^c	56 ± 9 ^c	52 ± 11 ^c	—	—	—

^aInsufficient time to map three participants.

^bInconsistent motor evoked potential (MEP) responses in three other participants.

^cOne child refused to perform JTTHF and BBT; hence, data of JTTHF and BBT represents mean ± SD of *n* = 28, *n* = 23, *n* = 14 in all children with UCP, contralesional M1-unaffected FDI map, and contralesional M1-affected FDI map, respectively.

unilateral motor mapping of the right hemisphere due to time constraints; one was excluded from analyses as their motor mapping intensity exceeded 100%MSO. Consistent MEP responses were induced in the contralateral left FDI (LFDI) when stimulating the right hemisphere in 21 TDC (88%), another 3 participants did not have consistent MEP responses.

Robust MEP responses were evoked in the contralateral, unaffected FDI during stimulation of the contralesional hemisphere in 24/29 participants with UCP (83%). MEP responses were evoked in the ipsilateral, affected FDI from stimulating the contralesional hemisphere in 15/29 children (52%), all of whom also had measurable responses in their unaffected hand to stimulation of the contralesional hemisphere. Five additional children (17%) had ipsilateral MEP present but insufficient responsive sites (<9) to create a map. Five children (15%) had robust MEP responses evoked in the affected FDI from stimulation of the lesioned M1 (see below). Table 2 characterizes the successfully derived maps and conditions that precluded the generation of maps in children with UCP.

3.3 | Contralesional motor maps of bilateral FDI in children with UCP

Representative contralesional hemisphere 2D maps and map overlay on MRI in children with UCP are depicted in Figure 2.

3.3.1 | Map area

Stimulation of the contralesional M1 generated a median unaffected FDI map area of 14.0 cm² (95% CI [8.8, 19.1], *n* = 24) and a median affected FDI map area of 14.2 cm² (95% CI [7.4, 17.6], *n* = 15). When comparing participants with bilateral FDI responses when stimulating the contralesional M1 (15/24), we observed that the unaffected FDI area was larger than the affected FDI area (*t* = 2.4, *p* = .03, Figure 3a).

3.3.2 | Peak MEP amplitude

Stimulation of the contralesional M1 generated a median peak MEP amplitude of 0.9 mV (95% CI [0.6, 1.3]) within the unaffected FDI map (*n* = 24) and a median peak MEP amplitude of 0.6 mV (95% CI [0.3, 1.2]) from the affected FDI map (*n* = 15). When comparing participants with bilateral FDI responses to stimulation of the contralesional M1 (15/24), a larger median peak MEP amplitude was observed in the unaffected FDI than that in the affected FDI (*W* = 72, *p* = .04, Figure 3b).

3.3.3 | Map volume

Stimulation of the contralesional M1 generated a median map volume of 4.9 mV cm² (95% CI [2.1, 8.2]) for the unaffected FDI (*n* = 24) and a median map volume of 3.6 mV cm² (95% CI [1.4, 6.0]) for the affected FDI (*n* = 15). When comparing participants with bilateral FDI responses when stimulating the contralesional M1 (15/24), we did not observe a difference in map volumes between the unaffected and affected FDI (*W* = 60, *p* = .09, Figure 3c).

3.4 | Contralesional motor maps compared to TDC

3.4.1 | Map area

Kruskal–Wallis test did not reveal significant differences in map area among groups (Kruskal–Wallis statistics = 2.43, *p* = .29). Stimulation of the left M1 in TDC generated RFDI maps with a median area of 11.3 cm² (95% CI [9.8, 13.2]) (*n* = 21). This was comparable to the median area of 14.0 cm² (95% CI [8.8, 19.1], *n* = 24) for both the unaffected (*p* = .41, Figure 3d) and the affected FDI area of 14.2 (95% CI [7.4, 17.6], *n* = 15) when stimulating the contralesional M1 in children with UCP (*p* = .83). No difference was observed between LFDI and RFDI map areas in TDC (*p* = .77).

TABLE 2 Demographics of motor map in participants with perinatal stroke and UCP

	Contralesional M1		Lesioned M1
	Unaffected FDI motor map	Affected FDI motor map	Affected FDI motor map
Motor map derived, <i>n</i> (%)	24 (82.8%)	15 (51.7%)	5 (17.2%)
No consistent MEP, <i>n</i> (%)	2 (6.9%)	7 (24.1%)	3 (10.3%)
No MEP responses, <i>n</i> (%)	2 (6.9%)	5 (17.2%)	18 (62.1%)
Unreliable baseline EMG signals, <i>n</i> (%)	1 (3.4%)	2 (6.9%)	2 (6.9%)
Time constraint to allow mapping, <i>n</i> (%)	0 (0%)	0 (0%)	1 (3.4%)
Resting motor threshold, mean (SD)	70.9 (5.6) %MSO ^a	74.1 (7.1) %MSO ^b	Unobtainable ^c

^aAveraged from 18 participants; 6 participants had RMT higher than 85%MSO.

^bAveraged from 13 participants; 2 participants had RMT higher than 85%MSO.

^cOnly one participant had measurable RMT at 74%MSO, the remaining four had RMT higher than 85%MSO.

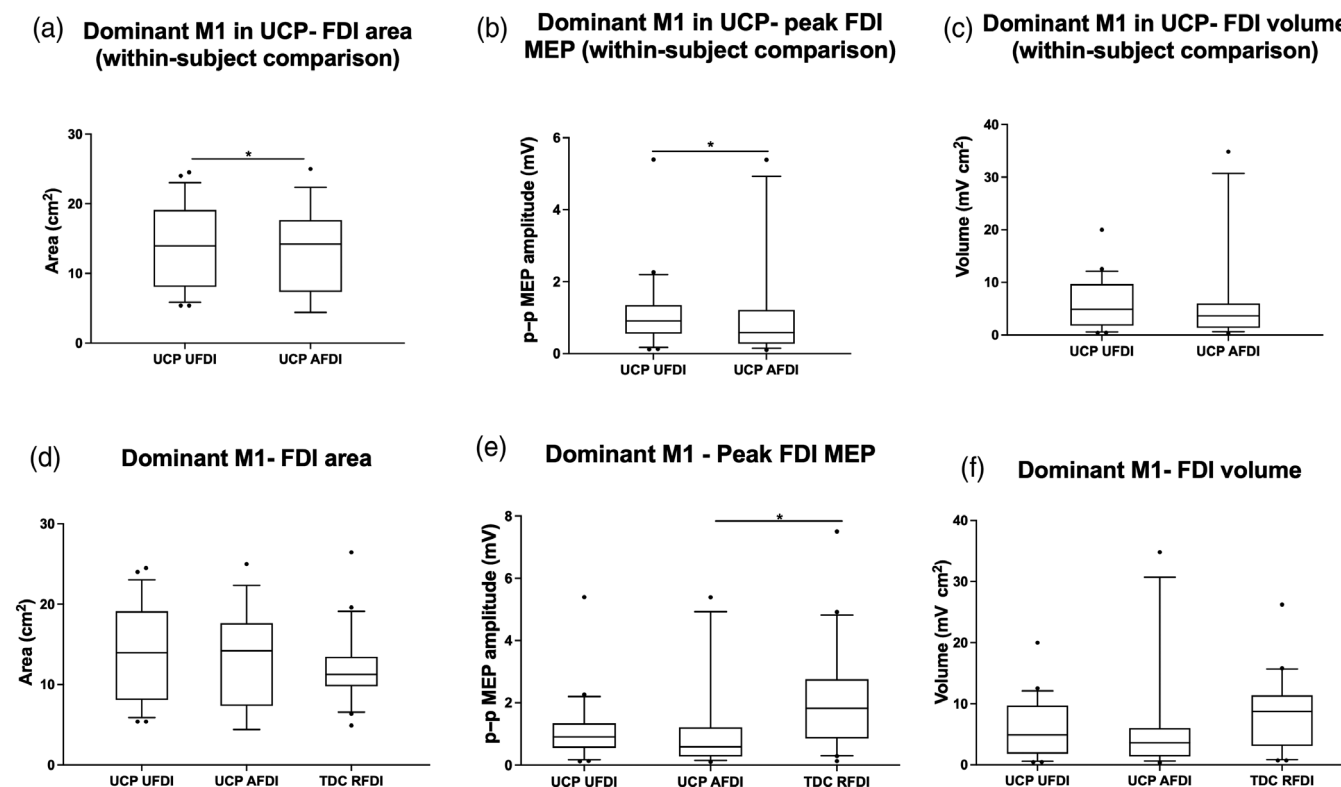


FIGURE 3 (a–c) Within-subject comparison in motor map outcome in children with UCP. (d–f) Group comparison in motor map outcome between children with perinatal stroke-induced UCP and TDC. (a) map area was larger in UFDI than AFDI. (b) Peak motor evoked potential (MEP) amplitude was larger in UFDI than AFDI. (c) No significant difference between affected and unaffected FDI volume. (d) No significant differences between TDC RFDI area and either FDI area in children with UCP. (e) Significant difference in peak MEP amplitude between TDC RFDI and AFDI in children with UCP. (f) No differences were observed in FDI volume between groups. AFDI, affected FDI; TDC, typically developing children; UCP, children with perinatal stroke-induced UCP; UFDI, unaffected FDI. Dominant M1 represents the contralesional motor cortex in children with perinatal stroke-induced UCP and left motor cortex in typically developing children. Box extends from 25 to 75th percentile and whiskers show 10–90th percentile

3.4.2 | Peak MEP amplitude

Kruskal–Wallis test revealed that there was a significant difference in peak MEP amplitude among groups (Kruskal–Wallis statistics = 7.23, $p = .03$). Stimulation of the left M1 generated a median peak MEP amplitude of 1.8 mV (95% CI [0.9, 2.7]) in the RFDI in TDC ($n = 21$). This was comparable to the median peak MEP amplitude of 0.9 mV (SD = 1.1, 95% CI [0.6, 1.3], $n = 24$) observed in the unaffected FDI when stimulating the contralesional M1 in children with UCP ($p = .15$, Figure 3e). Median peak MEP amplitude of 0.6 mV (SD = 1.6, 95% CI [0.3, 1.2], $n = 15$) in the affected FDI when stimulating the contralesional M1 in children with UCP was smaller than RFDI values in TDC ($p = .03$). We did not observe a difference between LFDI and RFDI peak MEP amplitudes in TDC ($p > .99$).

3.4.3 | Map volume

Kruskal–Wallis test did not reveal significant differences in map volume among groups (Kruskal–Wallis statistics = 4.42, $p = .11$). Stimulation of

the left M1 generated a median volume of 8.7 mV cm² (95% CI, [3.2, 11.2]) when MEP were recorded in the RFDI in TDC ($n = 21$). This was comparable to the median volume of 4.9 mV cm² (95% CI, [2.1, 8.2], $n = 24$) in the unaffected FDI ($p = .52$, Figure 3f) and the median volume of 3.6 mV cm² (95% CI [1.4, 6.0], $n = 15$) in the affected FDI when stimulating the contralesional M1 in children with UCP ($p = .12$). LFDI and RFDI volumes were comparable within TDC ($p = .63$).

3.5 | Nondominant M1 motor maps

The nondominant M1 refers to the lesioned M1 in children with UCP and right M1 in TDC. We used fMRI peak activation location as a guidance for optimizing stimulation target location for the lesioned hemisphere in 24/29 participants. Maps from the lesioned hemisphere could only be obtained in five subjects. Eighteen participants were excluded for no MEP response with the highest tolerable stimulation intensity; three were excluded for insufficient responsive sites (<9); two were excluded for unreliable baseline EMG signals. The 2D maps and map overlays on MRI are shown in Figure 4. Table 2 includes the

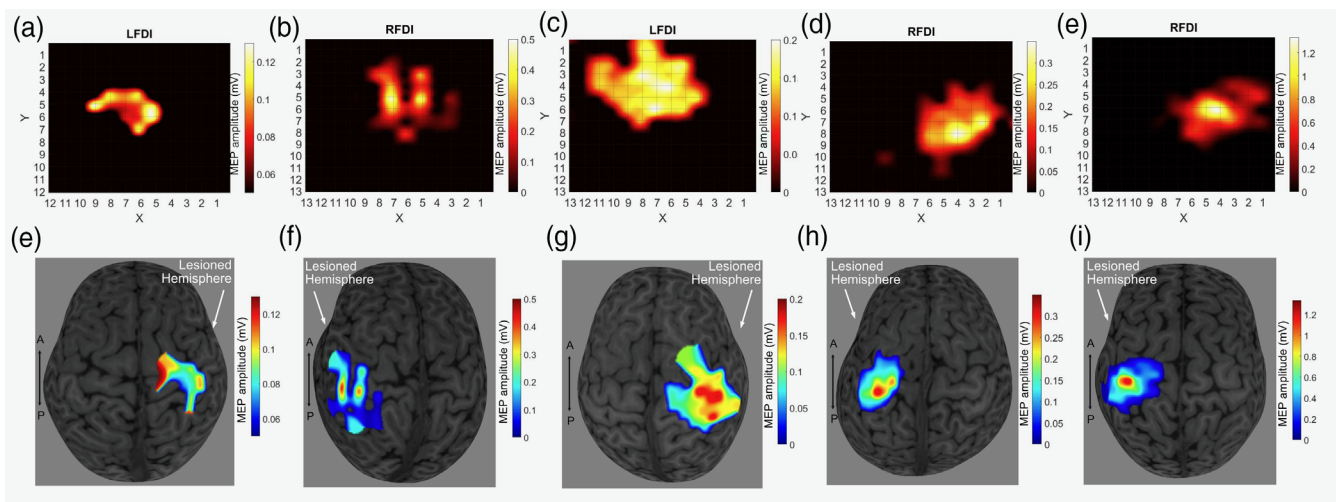


FIGURE 4 Lesioned hemisphere motor maps in children with perinatal stroke-induced unilateral cerebral palsy (UCP). (a–e): 2D heat maps of the affected first dorsal interosseus (FDI) from stimulating the lesioned motor cortex, (e–i) corresponding motor map overlap of the same participant in (a–e) on individual MRIs. Color bar on the right of individual figure represents the size of the motor evoked potential (MEP) amplitude

map details derived from stimulating the lesioned hemisphere in children with UCP.

3.5.1 | Map area

The median affected FDI map area from the lesioned M1 was 14.2 cm² (95% CI [5.9, 18.6], $n = 5$). By comparison, the median LFDI area was 11.3 cm² (95% CI [9.8, 13.7], $n = 21$) when stimulating the right M1 in TDC.

3.5.2 | Peak MEP amplitude

The median affected FDI peak MEP amplitude when mapping the lesioned M1 was 0.35 mV (95% CI [0.1, 1.3], $n = 5$). The median LFDI peak MEP amplitude from the right M1 in TDC was 1.4 mV (95% CI [0.9, 2.0], $n = 21$).

3.5.3 | Map volume

The median affected FDI volume when mapping the lesioned M1 was 2.3 mV cm² (95% CI [0.6, 6.0], $n = 5$) as compared to 5.6 mV cm² (95% CI [3.0, 11.8], $n = 21$) for the right M1 in TDC.

3.6 | Relationships between motor maps and clinical outcomes

For UCP participants with a valid contralesional M1 map ($n = 23$), the mean (SD) JTT of the affected hand was 225(206) s, the average BBT

score of the affected hand was 25(13) blocks/min, and the average AHA score was 55(16) logit units. TDC participants with valid left and right hemisphere maps ($n = 21$) had average right JTT of 28(5) s average left JTT of 31(5) s.

Unaffected FDI area was directly correlated with JTT of the unaffected hand (Figure 5a, Spearman's $r = -.58$, $p < .01$). This relationship remained significant when corrected for age (partial correlation = $-.48$, $p = .01$). Similarly, unaffected FDI peak MEP amplitude and volume were directly correlated with JTT of the unaffected hand (Figure 5b, Spearman's $r = -.50$, $p = .02$; Figure 5c, Spearman's $r = -.47$, $p = .02$). These relationships trended toward significance when corrected for age (partial correlation = $-.33$, $p = .07$; partial correlation = $-.35$, $p = .05$, respectively). In all the above correlations, higher values of mapping outcomes were associated with better hand function (lower score in the JTT). There were no other significant correlations between mapping and clinical outcomes.

3.7 | Safety and tolerability

During or immediately after the robotic TMS mapping session, the following were reported: headache (7, 24%; mild, $n = 5$, moderate, $n = 1$, severe, $n = 1$); neck pain (7, 24%; mild, $n = 5$, moderate, $n = 1$, severe, $n = 1$); tingling sensations (12, 41%); mild nausea (2, 7%); mild lightheaded (2, 7%). Participants ranked the robotic TMS session an average of 4th place; less favorable than common experiences such as “play a game,” “watch TV,” and “birthday party” but more favorable than experiences such as “go to a dentist” or “a long car ride” (Figure S1). Results of the safety and tolerability questionnaire for all TDC are previously published (Giuffre et al., 2021; Zewdie et al., 2020).

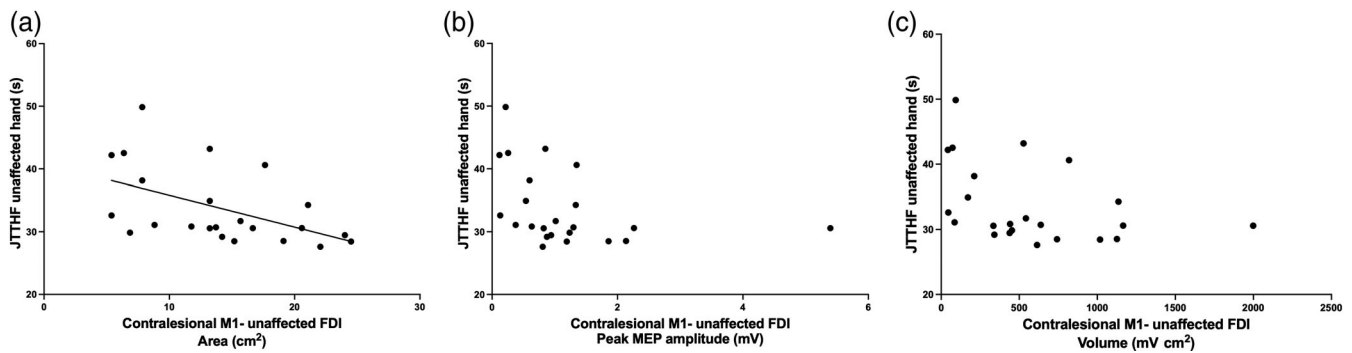


FIGURE 5 Correlations between motor mapping outcomes and Jebsen–Taylor Test of Hand Function (JTT). (a) Unaffected first dorsal interosseous (FDI) area was directly correlated with JTT of the unaffected hand, (b) unaffected FDI peak motor evoked potential (MEP) amplitude was correlated with JTT of the unaffected hand, (c) unaffected FDI volume was correlated with JTT of the unaffected hand. Note that the correlations in (b,c) trended toward significance when corrected for age (partial correlation = $-.33$, $p = .07$; partial correlation = $-.35$, $p = .05$, respectively)

4 | DISCUSSION

We demonstrate that robotic TMS motor mapping is feasible and safe in children with perinatal stroke and UCP. We were able to successfully generate unaffected FDI motor maps in 83% and affected FDI motor maps in 52% of children with UCP when stimulating the contralesional M1. Generating affected FDI maps from stimulation of the lesioned M1 was challenging, accomplished in only 17% of the sample. We found that the map area and peak MEP amplitude of the contralesional M1 representation of the affected FDI were both smaller as compared to the same parameters for the unaffected FDI. For peak MEP amplitude only, values were also smaller for the affected hand as compared to TDC. Correlations between all unaffected FDI motor map parameters and clinical function suggest clinical relevance for the dominant hand.

Motor maps have been investigated in animals and humans to better understand cortical neurophysiology and its relationship with function. Animal studies have demonstrated that skill training improvements may be accompanied by expansion of motor representations of the trained limbs (Kleim et al., 2002; Nudo, Milliken, et al., 1996; Nudo, Wise, et al., 1996). In adult stroke, it has been shown that motor interventions can enlarge motor map areas in association with functional improvements (Liepert, Bauder, et al. 2000; Liepert, Graef, et al. 2000; Sawaki et al., 2008). Recently, Friel et al. (2016) reported that map area and MEP amplitude showed differential changes when children with UCP were trained with intensive bimanual therapy.

Mapping of ipsilateral cortical representations of the affected hand is particularly relevant in children with UCP. Here, we observed that approximately 52% of children demonstrated a valid map of the affected FDI from stimulating the contralesional M1. This proportion is comparable to previous studies of perinatal stroke and other UCP populations undergoing corticospinal tract mapping with TMS where about half demonstrate such ipsilateral connections from the contralesional hemisphere (Smorenburg et al., 2017; Zewdie et al., 2017). Our results show how cortical motor maps might integrate into such

“pathway” oriented classifications of developmental plasticity after perinatal stroke (Hilderley et al., 2019; Kirton et al., 2021). Furthermore, addition of motor map characteristics to such models may provide new opportunities to study interventional plasticity in this population. Most existing noninvasive brain stimulation trials in children with UCP to date have targeted the contralesional M1 (Gillick et al., 2015, 2018; Kirton et al., 2016, 2017). Despite a similar approach, the rationale underlying this choice has varied with some based on the adult subcortical stroke model of interhemispheric imbalance while others advocate based on developmental models of contralesional control of spinal cord synapses. With both brain stimulation and intensive upper extremity therapies, a mechanistic understanding of the cortical control of the affected hand may help determine if such mechanisms are at play while identifying the shape and location of cortical targets for modulation.

Our findings of differences between the affected and unaffected FDI map characteristics add to recent studies exploring the underlying neurophysiology between the affected and the unaffected hands in children with UCP (Have et al., 2020; Rich et al., 2017). To date, most studies in this population have focused on the affected hand. However, the unaffected hand has also been shown to be impaired, including detailed robotic sensorimotor examinations in the perinatal stroke population (Kuczynski et al., 2018). Given that many children with UCP are severely impaired and rely heavily on the unaffected limb for daily function, understanding and even targeting this extremity for therapeutic intervention is considered but remains poorly studied. While we found differences in map area and peak MEP amplitude and correlations to motor outcomes, it is unclear how these neurophysiological measures relate to clinical function in individual patients. We also observed that the RMT of the affected and the unaffected FDI residing within the contralesional M1 may be different in children with UCP. In fact, four children had larger than 5%MSO difference in RMT between the affected and the unaffected FDI such that the contralesional M1 had to be mapped with two different stimulator intensities. This observation supports the importance of defining the RMT between each hand in children with UCP to help normalize mapping

outcomes to the excitability of the target muscle. Future studies exploring the relationship between the two motor maps within the contralesional hemisphere such as overlap may shed further light on underlying function.

The observation of no significant difference between the FDI area of either hand in children with UCP and the dominant FDI area in TDC was unexpected. Speculatively, the contralesional M1 in some children with UCP may potentially “take over” control of the affected hand to compensate for the lesioned M1. The degree to which this occurs is challenging to estimate as previous studies have shown a wide range of differences in such “laterality” and only modest correlations with clinical function (Friel et al., 2021; Kuo et al., 2021; Smorenburg et al., 2017). While the degree to which an ipsilateral map can be “installed” in the unintended, contralesional hemisphere is also not well defined and likely varies across individuals, that areas appear to fall within the normal range may indirectly support the occurrence of such developmental plasticity (Baker et al., 2020). This may be further supported by a sub-analysis showing that the unaffected FDI area from stimulating the contralesional M1 was larger than that of the left FDI when stimulating the right M1 in TDC.

In contrast, our findings of differences in the peak MEP amplitude between hands and the two groups are interesting. Friel et al. (2016) showed an increase in the overall MEP amplitude after motor learning in the structured group in children with UCP. Similarly, Nemanich et al. (2019) observed differential changes in the MEP amplitude in two groups children after receiving different therapies (active tDCS combined with constraint therapy vs. sham tDCS combined with constraint therapy). Recently, our group reported better correlations between subsets of mapping outcome (area and volume) and JTT in healthy adults (Giuffre et al., 2020, 2021). Briefly, this study showed decreased variabilities when using smaller subsets of mapping outcome as it contains larger MEPs of a motor map, when compared to using the entire map. Collectively, we speculate our findings here may suggest the peak of “3D-map mountain” to be an important biomarker and future studies may use such a simple metric to probe the underlying neurophysiology in children with UCP and TDC.

As the first study utilizing robotic TMS mapping in children with UCP, we found favorable safety and tolerability in support of future studies. Side effects reported were generally mild, self-limiting, and in keeping with what is now a large body of TMS safety data in children (Zewdie et al., 2020). Common experiences including tingling sensation, headache, and neck pain are expected but should be fully disclosed to participants and caregivers when obtaining informed consent. While rates appear similar to previously described CP and TDC populations, challenges for some children with UCP such as difficulty with attention or sitting still should be considered. While we had volunteers help support and protect children's head and provided breaks when necessary, the robotic coil requires a certain level of force feedback to ensure the contact between the coil and participants. Proper introduction, education, and orientation prior to initiating robotic TMS in children is recommended to optimize participant experience, compliance, and data collection.

Future directions include examining the application of robotic mapping in children with more severely affected CP as technology advances, and to understand the neurobiology of the motor maps in children with UCP and TDC as the goal of motor mapping research is to understand the neurophysiology and mechanisms associated with early brain injury and functional improvements. As robotic TMS has shown promising utility in providing details of neurophysiology, future studies would benefit from automatic mapping procedures to enhance experiment efficiency with established criteria. This technology may become a tool to obtain outcome as biomarkers to advance personalized rehabilitation in children with UCP.

Important limitations are acknowledged. First, the Axilum robotic TMS system only accommodates a 70-mm diameter biphasic Air-Film coil. The peak magnetic field strength (0.8T) is lower than that of other coils designed for neurophysiological evaluations (e.g., peak magnetic field of the Alpha Flat coil is >1.44T). This unmodifiable factor decreased our ability to obtain suprathreshold (and likely some rest threshold) MEP responses in our study, particularly given the known higher RMT in children and those with UCP, particularly in the lesioned hemisphere (Eyre et al., 2007; Rich et al., 2017; Smorenburg et al., 2017). Second, we may have underestimated motor map outcomes for the eight participants where stimulation of the contralesional M1 was unable to match the mapping intensity at 120% RMT (i.e., their RMT was >85%MSO). Similar phenomenon likely contributed to the challenges of mapping the lesioned M1. It is worthwhile considering this challenge of teasing apart whether the absence of MEPs when stimulating the lesioned hemisphere is due to true lack of cortical motor representation, insufficient stimulator intensity, or a combination of both. Other modalities, such as task-based fMRI, might be utilized to localize motor activation areas in the lesioned hemisphere when TMS fails to achieve localization of the hotspot. Third, we allowed children to watch movies as in other studies (Friel et al., 2021; Smorenburg et al., 2017) to ensure participants remained awake, steady, and interested throughout the experiment. While the movies were child-friendly, we would cautiously note that we cannot entirely exclude the effects of action observation on mapping physiology. Fourth, while the JTT, BBT, and AHA are standardized assessments, it is possible that we were not able to capture individual differences in discrete fine-motor movement quality using these outcomes. Finally, our sample size is relatively small compared to some adult studies though it represents the largest perinatal stroke study to date.

ACKNOWLEDGMENT

We thank children and families participating in this study, the staff support of following: the N3 network, the ACH Pediatric TMS laboratory, the PONI laboratory, and Drs. McMaster and Kiss laboratories. Hsing-Ching Kuo is funded by postdoctoral awards from the CPSR and ACHRI.

CONFLICT OF INTEREST

The authors declare that they have no conflicts of interest.

DATA AVAILABILITY STATEMENT

The data supporting the conclusions of this article will be made available by the authors.

ORCID

Hsing-Ching Kuo  <https://orcid.org/0000-0002-7019-7895>

Ephrem Zewdie  <https://orcid.org/0000-0003-1206-2471>

Adrianna Giuffre  <https://orcid.org/0000-0001-9632-0612>

Helen L. Carlson  <https://orcid.org/0000-0002-5788-0542>

James Wrightson  <https://orcid.org/0000-0001-7106-7470>

Adam Kirton  <https://orcid.org/0000-0001-5209-3374>

REFERENCES

- Araneda, R., Ebner-Karestinos, D., Paradis, J., Saussez, G., Friel, K. M., Gordon, A. M., & Bleyenheuft, Y. (2019). Reliability and responsiveness of the Jebsen-Taylor Test of Hand Function and the Box and Block Test for children with cerebral palsy. *Developmental Medicine and Child Neurology*, 61(10), 1182–1188. <https://doi.org/10.1111/dmcn.14184>
- Baker, K., Carlson, H. L., Zewdie, E., & Kirton, A. (2020). Developmental remodelling of the motor cortex in hemiparetic children with perinatal stroke. *Pediatric Neurology*, 112, 34–43. <https://doi.org/10.1016/j.pediatrneurol.2020.08.004>
- Beagley, S. B., Reedman, S. E., Sakzewski, L., & Boyd, R. N. (2016). Establishing Australian norms for the Jebsen Taylor Test of Hand Function in typically developing children aged five to 10 years: A pilot study. *Physical & Occupational Therapy in Pediatrics*, 36(1), 88–109. <https://doi.org/10.3109/01942638.2015.1040571>
- Cole, L., Dewey, D., Letourneau, N., Kaplan, B. J., Chaput, K., Gallagher, C., Hodge, J., Floer, A., & Kirton, A. (2017). Clinical characteristics, risk factors, and outcomes associated with neonatal hemorrhagic stroke: A population-based case-control study. *JAMA Pediatrics*, 171(3), 230–238. <https://doi.org/10.1001/jamapediatrics.2016.4151>
- Cole, L., Giuffre, A., Ciecchanski, P., Carlson, H. L., Zewdie, E., Kuo, H.-C., & Kirton, A. (2018). Effects of high-definition and conventional transcranial direct-current stimulation on motor learning in children. *Frontiers in Neuroscience*, 12, 787. <https://doi.org/10.3389/fnins.2018.00787>
- Craig, B. T., Hilderley, A., Kinney-Lang, E., Long, X., Carlson, H. L., & Kirton, A. (2020). Developmental neuroplasticity of the white matter connectome in children with perinatal stroke. *Neurology*, 95(18), e2476–e2486. <https://doi.org/10.1212/WNL.0000000000010669>
- Dunbar, M., & Kirton, A. (2018). Perinatal stroke: Mechanisms, management, and outcomes of early cerebrovascular brain injury. *The Lancet. Child & Adolescent Health*, 2(9), 666–676. [https://doi.org/10.1016/S2352-4642\(18\)30173-1](https://doi.org/10.1016/S2352-4642(18)30173-1)
- Dunbar, M., & Kirton, A. (2019). Perinatal Stroke. *Seminars in Pediatric Neurology*, 32, 100767. <https://doi.org/10.1016/j.spn.2019.08.003>
- Dunbar, M., Mineyko, A., Hill, M., Hodge, J., Floer, A., & Kirton, A. (2020). Population based birth prevalence of disease-specific perinatal stroke. *Pediatrics*, 146(5), e2020013201. <https://doi.org/10.1542/peds.2020-013201>
- Duncan, P., Richards, L., Wallace, D., Stoker-Yates, J., Pohl, P., Luchies, C., Ogle, A., & Studenski, S. (1998). A randomized, controlled pilot study of a home-based exercise program for individuals with mild and moderate stroke. *Stroke*, 29(10), 2055–2060. <https://doi.org/10.1161/01.STR.29.10.2055>
- Eyre, J. A., Smith, M., Dabydeen, L., Clowry, G. J., Petacchi, E., Battini, R., Guzzetta, A., & Cioni, G. (2007). Is hemiplegic cerebral palsy equivalent to amblyopia of the corticospinal system? *Annals of Neurology*, 62(5), 493–503. <https://doi.org/10.1002/ana.21108>
- Friel, K., Chakrabarty, S., Kuo, H.-C., & Martin, J. (2012). Using motor behavior during an early critical period to restore skilled limb movement after damage to the corticospinal system during development. *Journal of Neuroscience*, 32(27), 9265–9276. <https://doi.org/10.1523/JNEUROSCI.1198-12.2012>
- Friel, K. M., Ferre, C. L., Brandao, M., Kuo, H.-C., Chin, K., Hung, Y.-C., Robert, M. T., Flamand, V. H., Smorenburg, A., Bleyenheuft, Y., Carmel, J. B., Campos, T., & Gordon, A. M. (2021). Improvements in upper extremity function following intensive training are independent of corticospinal tract organization in children with unilateral spastic cerebral palsy: A clinical randomized trial. *Frontiers in Neurology*, 12, 660780. <https://doi.org/10.3389/fneur.2021.660780>
- Friel, K. M., Heddings, A. A., & Nudo, R. J. (2000). Effects of postlesion experience on behavioral recovery and neurophysiologic reorganization after cortical injury in primates. *Neurorehabilitation and Neural Repair*, 14(3), 187–198. <https://doi.org/10.1177/154596830001400304>
- Friel, K. M., Kuo, H.-C., Fuller, J., Ferre, C. L., Brandão, M., Carmel, J. B., Bleyenheuft, Y., Gowatsky, J. L., Stanford, A. D., Rowny, S. B., Lubner, B., Bassi, B., Murphy, D. L. K., Lisanby, S. H., & Gordon, A. M. (2016). Skilled bimanual training drives motor cortex plasticity in children with unilateral cerebral palsy. *Neurorehabilitation and Neural Repair*, 30(9), 834–844. <https://doi.org/10.1177/1545968315625838>
- Garvey, M. A., Kaczynski, K. J., Becker, D. A., & Bartko, J. J. (2001). Subjective reactions of children to single-pulse transcranial magnetic stimulation. *Journal of Child Neurology*, 16(12), 891–894. <https://doi.org/10.1177/088307380101601205>
- Gillick, B., Menk, J., Mueller, B., Meekins, G., Krach, L. E., Feyma, T., & Rudser, K. (2015). Synergistic effect of combined transcranial direct current stimulation/constraint-induced movement therapy in children and young adults with hemiparesis: Study protocol. *BMC Pediatrics*, 15, 178. <https://doi.org/10.1186/s12887-015-0498-1>
- Gillick, B., Rich, T., Nemanich, S., Chen, C.-Y., Menk, J., Mueller, B., Chen, M., Ward, M., Meekins, G., Feyma, T., Krach, L., & Rudser, K. (2018). Transcranial direct current stimulation and constraint-induced therapy in cerebral palsy: A randomized, blinded, sham-controlled clinical trial. *European Journal of Paediatric Neurology: EJPN*, 22(3), 358–368. <https://doi.org/10.1016/j.ejpn.2018.02.001>
- Giuffre, A., Cole, L., Kuo, H.-C., Carlson, H. L., Grab, J., Kirton, A., & Zewdie, E. (2019). Non-invasive modulation and robotic mapping of motor cortex in the developing brain. *Journal of Visualized Experiments: JoVE*, 149. <https://doi.org/10.3791/59594>
- Giuffre, A., Kahl, C. K., Zewdie, E., Wrightson, J. G., Bourgeois, A., Condliffe, E. G., & Kirton, A. (2020). Reliability of robotic transcranial magnetic stimulation motor mapping. *Journal of Neurophysiology*, 125(1), 74–85. <https://doi.org/10.1152/jn.00527.2020>
- Giuffre, A., Zewdie, E., Carlson, H. L., Wrightson, J. G., Kuo, H.-C., Cole, L., & Kirton, A. (2021). Robotic transcranial magnetic stimulation motor maps and hand function in adolescents. *Physiological Reports*, 9(7), e14801. <https://doi.org/10.14814/phy2.14801>
- Goetz, S., Cassie Kozyrkov, I., Lubner, B., Lisanby, S. H., Murphy, D. L., Grill, W. M., & Peterchev, A. V. (2019). Accuracy of robotic coil positioning during transcranial magnetic stimulation. *Journal of Neural Engineering*, 16, 054003. <https://doi.org/10.1088/1741-2552/ab2953>
- Grab, J. G., Zewdie, E., Carlson, H. L., Kuo, H. C., Ciecchanski, P., Hodge, J., Giuffre, A., & Kirton, A. (2018). Robotic TMS mapping of motor cortex in the developing brain. *Journal of Neuroscience Methods*, 309, 41–54. <https://doi.org/10.1016/j.jneumeth.2018.08.007>
- Grefkes, C., & Ward, N. S. (2014). Cortical reorganization after stroke: How much and how functional? *The Neuroscientist*, 20(1), 56–70. <https://doi.org/10.1177/1073858413491147>
- Hawe, R. L., Kuczynski, A. M., Kirton, A., & Dukelow, S. P. (2020). Assessment of bilateral motor skills and visuospatial attention in children with perinatal stroke using a robotic object hitting task. *Journal of Neuroengineering and Rehabilitation*, 17(1), 18. <https://doi.org/10.1186/s12984-020-0654-1>
- Hilderley, A. J., Metzler, M. J., & Kirton, A. (2019). Noninvasive neuromodulation to promote motor skill gains after perinatal stroke.

- Stroke, 50(2), 233–239. <https://doi.org/10.1161/STROKEAHA.118.020477>
- Jebsen, R. H., Taylor, N., Trieschmann, R. B., Trotter, M. J., & Howard, L. A. (1969). An objective and standardized test of hand function. *Archives of Physical Medicine and Rehabilitation*, 50(6), 311–319.
- Jongbloed-Pereboom, M., Maria, W. G., der Sanden, N.-v., & Steenbergen, B. (2013). Norm scores of the Box and Block Test for children ages 3–10 years. *The American Journal of Occupational Therapy: Official Publication of the American Occupational Therapy Association*, 67(3), 312–318. <https://doi.org/10.5014/ajot.2013.006643>
- Juenger, H., Kuhnke, N., Braun, C., Ummenhofer, F., Wilke, M., Walther, M., Koerte, I., Delvendahl, I., Jung, N. H., Berweck, S., Staudt, M., & Mall, V. (2013). Two types of exercise-induced neuroplasticity in congenital hemiparesis: A transcranial magnetic stimulation, functional MRI, and magnetoencephalography study. *Developmental Medicine and Child Neurology*, 55(10), 941–951. <https://doi.org/10.1111/dmcn.12209>
- Kesar, T. M., Sawaki, L., Burdette, J. H., Cabrera, M. N., Kolaski, K., Smith, B. P., O'Shea, T. M., Koman, L. A., & Wittenberg, G. F. (2012). Motor cortical functional geometry in cerebral palsy and its relationship to disability. *Clinical Neurophysiology: Official Journal of the International Federation of Clinical Neurophysiology*, 123(7), 1383–1390. <https://doi.org/10.1016/j.clinph.2011.11.005>
- Kirton, A., Andersen, J., Herrero, M., Nettel-Aguirre, A., Carsolio, L., Damji, O., Keess, J., Mineyko, A., Hodge, J., & Hill, M. D. (2016). Brain stimulation and constraint for perinatal stroke hemiparesis: The plastic champs trial. *Neurology*, 86(18), 1659–1667. <https://doi.org/10.1212/WNL.0000000000002646>
- Kirton, A., Ciecchanski, P., Zewdie, E., Andersen, J., Nettel-Aguirre, A., Carlson, H., Carsolio, L., Herrero, M., Quigley, J., Mineyko, A., Hodge, J., & Hill, M. (2017). Transcranial direct current stimulation for children with perinatal stroke and hemiparesis. *Neurology*, 88(3), 259–267. <https://doi.org/10.1212/WNL.0000000000003518>
- Kirton, A., & Deveber, G. (2013). Life after perinatal stroke. *Stroke*, 44(11), 3265–3271. <https://doi.org/10.1161/STROKEAHA.113.000739>
- Kirton, A., Metzler, M. J., Craig, B. T., Hilderley, A., Dunbar, M., Giuffre, A., Wrightson, J., Zewdie, E., & Carlson, H. L. (2021). Perinatal stroke: mapping and modulating developmental plasticity. *Nature Reviews. Neurology*, 17(7), 415–432. <https://doi.org/10.1038/s41582-021-00503-x>
- Kleim, J. A., Barbay, S., & Nudo, R. J. (1998). Functional reorganization of the rat motor cortex following motor skill learning. *Journal of Neurophysiology*, 80(6), 3321–3325. <https://doi.org/10.1152/jn.1998.80.6.3321>
- Kleim, J. A., Barbay, S., Cooper, N. R., Hogg, T. M., Reidel, C. N., Remple, M. S., & Nudo, R. J. (2002). Motor learning-dependent synaptogenesis is localized to functionally reorganized motor cortex. *Neurobiology of Learning and Memory*, 77(1), 63–77. <https://doi.org/10.1006/nlme.2000.4004>
- Krumlinde-Sundholm, L., Holmfur, M., Kottorp, A., & Eliasson, A.-C. (2007). The assisting hand assessment: Current evidence of validity, reliability, and responsiveness to change. *Developmental Medicine and Child Neurology*, 49(4), 259–264. <https://doi.org/10.1111/j.1469-8749.2007.00259.x>
- Kuczynski, A. M., Kirton, A., Semrau, J. A., & Dukelow, S. P. (2018). Bilateral reaching deficits after unilateral perinatal ischemic stroke: A population-based case-control study. *Journal of Neuroengineering and Rehabilitation*, 15(1), 77. <https://doi.org/10.1186/s12984-018-0420-9>
- Kuo, H.-C., Ferre, C. L., Carmel, J. B., Gowatsky, J. L., Stanford, A. D., Rowny, S. B., Lisanby, S. H., Gordon, A. M., & Friel, K. M. (2017). Using diffusion tensor imaging to identify corticospinal tract projection patterns in children with unilateral spastic cerebral palsy. *Developmental Medicine and Child Neurology*, 59(1), 65–71. <https://doi.org/10.1111/dmcn.13192>
- Kuo, H.-C., Friel, K. M., & Gordon, A. M. (2018). Neurophysiological mechanisms and functional impact of mirror movements in children with unilateral spastic cerebral palsy. *Developmental Medicine and Child Neurology*, 60(2), 155–161. <https://doi.org/10.1111/dmcn.13524>
- Kuo, H.-C., Litzenberger, J., Nettel-Aguirre, A., Zewdie, E., & Kirton, A. (2021). Exploring clinical and neurophysiological factors associated with response to constraint therapy and brain stimulation in children with hemiparetic cerebral palsy. *Developmental Neurorehabilitation*, 25(4), 229–238.
- Liepert, J., Bauder, H., Wolfgang, H. R., Miltner, W. H., Taub, E., & Weiller, C. (2000). Treatment-induced cortical reorganization after stroke in humans. *Stroke*, 31(6), 1210–1216. <https://doi.org/10.1161/01.str.31.6.1210>
- Liepert, J., Graef, S., Uhde, I., Leidner, O., & Weiller, C. (2000). Training-induced changes of motor cortex representations in stroke patients. *Acta Neurologica Scandinavica*, 101(5), 321–326. <https://doi.org/10.1034/j.1600-0404.2000.90337a.x>
- Marneweck, M., Kuo, H.-C., Smorenburg, A. R. P., Ferre, C. L., Flamand, V. H., Gupta, D., Carmel, J. B., Bleyenheuft, Y., Gordon, A. M., & Friel, K. M. (2018). The relationship between hand function and overlapping motor representations of the hands in the contralesional hemisphere in unilateral spastic cerebral palsy. *Neurorehabilitation and Neural Repair*, 32(1), 62–72. <https://doi.org/10.1177/1545968317745991>
- Martin, J. H., Chakrabarty, S., & Friel, K. M. (2011). Harnessing activity-dependent plasticity to repair the damaged corticospinal tract in an animal model of cerebral palsy. *Developmental Medicine & Child Neurology*, 53(s4), 9–13. <https://doi.org/10.1111/j.1469-8749.2011.04055.x>
- Martin, J. H., Friel, K. M., Salimi, I., & Chakrabarty, S. (2007). Activity- and use-dependent plasticity of the developing corticospinal system. *Neuroscience and Biobehavioral Reviews*, 31(8), 1125–1135. <https://doi.org/10.1016/j.neubiorev.2007.04.017>
- Mathiowetz, V., Volland, G., Kashman, N., & Weber, K. (1985). Adult norms for the box and block test of manual dexterity. *The American Journal of Occupational Therapy*, 39(6), 386–391. <https://doi.org/10.5014/ajot.39.6.386>
- Milliken, G. W., Plautz, E. J., & Nudo, R. J. (2013). Distal forelimb representations in primary motor cortex are redistributed after forelimb restriction: A longitudinal study in adult squirrel monkeys. *Journal of Neurophysiology*, 109(5), 1268–1282. <https://doi.org/10.1152/jn.00044.2012>
- Nemanich, S. T., Rich, T. L., Chen, C.-Y., Menk, J., Rudser, K., Chen, M., Meekins, G., & Gillick, B. T. (2019). Influence of combined transcranial direct current stimulation and motor training on corticospinal excitability in children with unilateral cerebral palsy. *Frontiers in Human Neuroscience*, 13, 137. <https://doi.org/10.3389/fnhum.2019.00137>
- Nudo, R. J., & Milliken, G. W. (1996). Reorganization of movement representations in primary motor cortex following focal ischemic infarcts in adult squirrel monkeys. *Journal of Neurophysiology*, 75(5), 2144–2149. <https://doi.org/10.1152/jn.1996.75.5.2144>
- Nudo, R. J., Milliken, G. W., Jenkins, W. M., & Merzenich, M. M. (1996). Use-dependent alterations of movement representations in primary motor cortex of adult squirrel monkeys. *The Journal of Neuroscience: The Official Journal of the Society for Neuroscience*, 16(2), 785–807.
- Nudo, R. J., Wise, B. M., SiFuentes, F., & Milliken, G. W. (1996). Neural substrates for the effects of rehabilitative training on motor recovery after ischemic infarct. *Science*, 272(5269), 1791–1794. <https://doi.org/10.1126/science.272.5269.1791>
- Oskoui, M., Coutinho, F., Dykeman, J., Jetté, N., & Pringsheim, T. (2013). An update on the prevalence of cerebral palsy: A systematic review and meta-analysis. *Developmental Medicine and Child Neurology*, 55(6), 509–519. <https://doi.org/10.1111/dmcn.12080>
- Penfield, W., & Rasmussen, T. (1950). *The cerebral cortex of man: A clinical study of localization of function*. Macmillan.

- Raju, T. N. K., Nelson, K. B., Ferriero, D., Lynch, J. K., & NICHD-NINDS Perinatal Stroke Workshop Participants. (2007). Ischemic perinatal stroke: Summary of a Workshop sponsored by the National Institute of Child Health and Human Development and the National Institute of Neurological Disorders and Stroke. *Pediatrics*, 120(3), 609–616. <https://doi.org/10.1542/peds.2007-0336>
- Reedman, S. E., Beagley, S., Sakzewski, L., & Boyd, R. N. (2016). The Jebsen Taylor Test of Hand Function: A pilot test-retest reliability study in typically developing children. *Physical & Occupational Therapy in Pediatrics*, 36(3), 292–304. <https://doi.org/10.3109/01942638.2015.1040576>
- Rich, T. L., Menk, J. S., Rudser, K. D., Feyma, T., & Gillick, B. T. (2017). Less-affected hand function in children with Hemiparetic unilateral cerebral palsy: A comparison study with typically developing peers. *Neurorehabilitation and Neural Repair*, 31(10–11), 965–976. <https://doi.org/10.1177/1545968317739997>
- Riddell, M., Kuo, H.-C., Zewdie, E., & Kirton, A. (2019). Mirror movements in children with unilateral cerebral palsy due to perinatal stroke: Clinical correlates of plasticity reorganization. *Developmental Medicine and Child Neurology*, 61(8), 943–949. <https://doi.org/10.1111/dmcn.14155>
- Sawaki, L., Butler, A. J., Leng, X., Wassenaar, P. A., Mohammad, Y. M., Blanton, S., Sathian, K., Nichols-Larsen, D. S., Wolf, S. L., Good, D. C., & Wittenberg, G. F. (2008). Constraint-induced movement therapy results in increased motor map area in subjects 3 to 9 months after stroke. *Neurorehabilitation and Neural Repair*, 22(5), 505–513. <https://doi.org/10.1177/1545968308317531>
- Simon-Martinez, C., Jaspers, E., Alaerts, K., Ortibus, E., Balsters, J., Mailloux, L., Blommaert, J., Sleurs, C., Klingels, K., Amant, F., Uyttebroeck, A., Wenderoth, N., & Feys, H. (2019). Influence of the corticospinal tract wiring pattern on sensorimotor functional connectivity and clinical correlates of upper limb function in unilateral cerebral palsy. *Scientific Reports*, 9(1), 8230. <https://doi.org/10.1038/s41598-019-44728-9>
- Smorenburg, A. R. P., Gordon, A. M., Kuo, H.-C., Ferre, C. L., Brandao, M., Bleyenheuft, Y., Carmel, J. B., & Friel, K. M. (2017). Does corticospinal tract connectivity influence the response to intensive bimanual therapy in children with unilateral cerebral palsy? *Neurorehabilitation and Neural Repair*, 31(3), 250–260. <https://doi.org/10.1177/1545968316675427>
- Staudt, M. (2007). Reorganization of the developing human brain after early lesions. *Developmental Medicine and Child Neurology*, 49(8), 564. <https://doi.org/10.1111/j.1469-8749.2007.00564.x>
- Taylor, N., Sand, P. L., & Jebsen, R. H. (1973). Evaluation of hand function in children. *Archives of Physical Medicine and Rehabilitation*, 54(3), 129–135.
- Thickbroom, G. W., Byrnes, M. L., Archer, S. A., & Mastaglia, F. L. (2004). Motor outcome after subcortical stroke correlates with the degree of cortical reorganization. *Clinical Neurophysiology*, 115(9), 2144–2150. <https://doi.org/10.1016/j.clinph.2004.04.001>
- Wu, Y. W., Lindan, C. E., Henning, L. H., Yoshida, C. K., Fullerton, H. J., Ferriero, D. M., James Barkovich, A., & Croen, L. A. (2006). Neuroimaging abnormalities in infants with congenital hemiparesis. *Pediatric Neurology*, 35(3), 191–196. <https://doi.org/10.1016/j.pediatrneurol.2006.03.002>
- Yarossi, M., Patel, J., Qiu, Q., Massood, S., Fluet, G., Merians, A., Adamovich, S., & Tunik, E. (2019). The association between reorganization of bilateral M1 topography and function in response to early intensive hand focused upper limb rehabilitation following stroke is dependent on ipsilesional corticospinal tract integrity. *Frontiers in Neurology*, 10, 258. <https://doi.org/10.3389/fneur.2019.00258>
- Zewdie, E., Ciecchanski, P., Kuo, H. C., Giuffre, A., Kahl, C., King, R., Cole, L., Godfrey, H., Seeger, T., Swansburg, R., Damji, O., Rajapakse, T., Hodge, J., Nelson, S., Selby, B., Gan, L., Jadavji, Z., Larson, J. R., MacMaster, F., ... Kirton, A. (2020). Safety and tolerability of transcranial magnetic and direct current stimulation in children: Prospective single center evidence from 3.5 million stimulations. *Brain Stimulation*, 13(3), 565–575. <https://doi.org/10.1016/j.brs.2019.12.025>
- Zewdie, E., Damji, O., Ciecchanski, P., Seeger, T., & Kirton, A. (2017). Contralateral corticomotor neurophysiology in hemiparetic children with perinatal stroke. *Neurorehabilitation and Neural Repair*, 31(3), 261–271. <https://doi.org/10.1177/1545968316680485>

SUPPORTING INFORMATION

Additional supporting information may be found in the online version of the article at the publisher's website.

How to cite this article: Kuo, H.-C., Zewdie, E., Giuffre, A., Gan, L. S., Carlson, H. L., Wrightson, J., & Kirton, A. (2022). Robotic mapping of motor cortex in children with perinatal stroke and hemiparesis. *Human Brain Mapping*, 43(12), 3745–3758. <https://doi.org/10.1002/hbm.25881>